BASIC RESEARCH

Comparison of two peptide radiotracers for prostate carcinoma targeting

Bluma Linkowski Faintuch,[I] Erica A. Oliveira,[I] Eutimio G. F. Nunez,[I] Ana M. Moro,[II] P. K. Nanda,[III] Charles J. Smith[III]

[I]Institute of Energy and Nuclear Research, (IPEN/CNEN), Radiopharmacy Center, São Paulo, Brazil. [II]Butantan Institute, Laboratory of Monoclonal Antibodies, São Paulo, SP, Brazil. [III]University of Missouri, School of Medicine, Department of Radiology, Columbia, MO, USA.

OBJECTIVES: Scintigraphy is generally not the first choice treatment for prostate cancer, although successful studies using bombesin analog radiopeptides have been performed. Recently, a novel peptide obtained using a phage display library demonstrated an affinity for prostate tumor cells. The aim of this study was to compare the use of a bombesin analog to that of a phage display library peptide (DUP-1) radiolabeled with technetium-99m for the treatment of prostate carcinoma. The peptides were first conjugated to S-acetyl-MAG3 with a 6-carbon spacer, namely aminohexanoic acid.

METHODS: The technetium-99m labeling required a sodium tartrate buffer. Radiochemical evaluation was performed using ITLC and was confirmed by high-performance liquid chromatography. The coefficient partition was determined, and *in vitro* studies were performed using human prostate tumor cells. Biodistribution was evaluated in healthy animals at various time points and also in mice bearing tumors.

RESULTS: The radiochemical purity of both radiotracers was greater than 95%. The DUP-1 tracer was more hydrophilic (*log* P = -2.41) than the bombesin tracer (*log* P = -0.39). The biodistribution evaluation confirmed this hydrophilicity by revealing the greater kidney uptake of DUP-1. The bombesin concentration in the pancreas was greater than that of DUP-1 due to specific gastrin-releasing peptide receptors. Bombesin internalization occurred for 78.32% of the total binding in tumor cells. The DUP-1 tracer showed very low binding to tumor cells during the *in vitro* evaluation, although tumor uptake for both tracers was similar. The tumors were primarily blocked by DUP-1 and the bombesin radiotracer primarily targeted the pancreas.

CONCLUSION: Further studies with the radiolabeled DUP-1 peptide are recommended. With further structural changes, this molecule could become an efficient alternative tracer for prostate tumor diagnosis.

KEYWORDS: Bombesin; DUP-1 Peptide; Technetium-99m; Prostate Tumor; Radiolabeling.

Faintuch BL, Oliveira EA, Nunez EGF, Moro AM, Nanda PK, Smith CJ. Comparison of two peptide radiotracers for prostate carcinoma targeting. Clinics. 2012;67(2):163-170.

Received for publication on July 24, 2011; **First review completed on** August 23, 2011; **Accepted for publication on** September 5, 2011

E-mail: blfaintuch@hotmail.com

Tel.: 55 11 31339531

INTRODUCTION

Many investigations have been conducted using diagnostic radiotracers specific for prostate cancer, as prostate cancer is a condition characterized by substantial morbidity and mortality. Radiolabeled bombesin analog are preferable because they target gastrin-releasing peptide receptor (GRPR)-expressing tumors (1-2). GRPR is highly expressed on the surface of malignant human prostate cells, and its specificity for prostate cancer, compared to benign hyperplastic prostate tissue, has been demonstrated (3-5).

No potential conflict of interest was reported.

Bombesin (BBN) is a 14-amino acid neuropeptide that was isolated from the skin of the European *Bombina* frog, and it shows a high affinity for the gastrin-releasing peptide receptor. BBN and its mammalian homolog, GRP, share a seven-amino-acid sequence in their C-terminal region, which is essential for receptor binding and biological activity (6,7).

Most studies that have used radiolabeled BBN have focused on prostate cancer, although some have also focused on breast cancer (8,9). Recent efforts in the field of phage display technology have led to significant drug discoveries. Phage display peptide libraries encompass high-affinity molecules that show potential for use in cancer diagnosis (10).

The synthetic peptide FRPNRAQDYNTN (DUP-1) was identified by phage display techniques. The DUP-1 peptide binds to DU-145 prostate cells and also to PC-3 cells with high affinity (11).

DUP-1 has been radiolabeled with iodine-131 (11) and also recently with indium-111 (^{111}In) (12). However, no

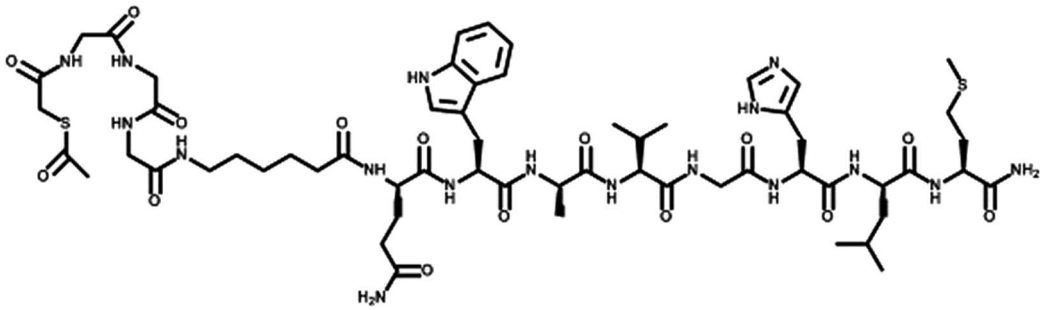

Figure 1 - Structure of conjugated bombesin (SAMA-G-G-G-Ahx-QWAVGHLM-NH2); chemical formula: $C_{59}H_{89}N_{17}O_{15}S_2$; molecular weight: 1340.57.

reports have focused on the use of one of the most widely used SPECT radioisotopes, technetium-99m (^{99m}Tc).

Askoxilakis et al. (12) demonstrated that the phage display linear molecule DUP-1 is generally serum-instable, which suggests the existence of targeted modifications, such as cyclization, an exchange of amino acids, such D-amino acids, and peptide acetylation.

Technetium-99m (^{99m}Tc) has many advantages, including its widespread availability, low cost and convenient physicochemical properties, such as its half-life ($t_{1/2} = 6$ h) and gamma energy ($E\gamma = 140$ keV). Moreover, it can also be provided as part of a ready-to-use lyophilized kit. Different approaches have been used to label biomolecules with ^{99m}Tc by means of bifunctional chelators, including hydrazine-nicotinic acid (HYNIC) or mercaptoacetylglycyltriglycine (MAG3). The use of preformed metallic precursors, such as organometallic ^{99m}Tc(CO)$_3$ or ^{99m}Tc-nitrido, as well as the 3+1 or 4+1 mixed ligand approach and the ''click chemistry'' procedure are additional approaches used for labeling (13). The S-acetyl NHS-MAG3 chelator was originally used for the post-conjugation labeling of antibodies, peptides and oligomers with ^{99m}Tc; this is typically performed at a neutral pH and at room temperature.

The aim of this study was to compare the use of a bombesin analog to that of a phage display peptide (DUP-1) labeled with technetium-99m for experimental prostate carcinoma. PC3 human prostate cancer cells were used in this study, and these represent an attractive target for bombesin markers because they overexpress GRPR. Schally and co-workers have further shown that there are 44,000 bombesin receptor sites/cell on PC-3 human prostate cancer cells (14).

The peptides were conjugated with S-acetyl mercaptoacetyl-triglycine (SAMA-G3) using a six-carbon spacer, namely aminohexanoic acid (Figs. 1 and 2). It was hypothesized that both the classic bombesin tracer as well as the DUP-1 tracer would be confirmed as potential tools for nuclear medicine diagnoses.

MATERIALS AND METHODS

Materials

All of the chemicals used were reagent-grade (Sigma-Aldrich and Merck, São Paulo, Brazil). The peptide-conjugated bombesin analog (SAMA-G-G-G-Ahx-QWAVGHLM-NH2, abbreviated as SAMA-G3-Ahx-BBN) and the phage display peptide DUP-1 (FRPNRAQDYNTNK-SAMA-G-G-G-Ahx-NH2, abbreviated as SAMA-G3-Ahx-DUP-1) (Figures 1, 2) were purchased from piChem Laboratory (Graz, Austria).

^{99m}Tc, in the form of Na^{99m}TcO$_4$, was eluted in saline from an alumina-based ^{99}Mo/^{99m}Tc generator, which was supplied by the Institute of Energetic and Nuclear Research/Brazilian Commission of Nuclear Energy (IPEN/CNEN, São Paulo, Brazil). Silica gel strips (ITLC-SG, Gelman Science, Ann Arbor, MI, USA) were used for instant thin-layer chromatography. Reverse-phase high-performance liquid chromatography (RP-HPLC, Shimadzu, Kyoto, Japan) was also performed using a Symmetry C-18 column (5.0 μm, 100 Å, 4.6×250 mm, Waters, Milford, MA, USA).

Radioactivity measurements were conducted using an automated, well-typed γ-counter NaI(Tl) crystal (Canberra, Meriden, CT, USA). The PC-3 human prostate adenocarcinoma cell line was obtained from the American Type Culture Collection (ATCC, Manassas, VA, USA). Male Swiss albino mice (20 - 25 g) and male nude mice (16 - 20 g) were used for the biodistribution studies, and the animals were provided by the Animal Facility of IPEN/CNEN in São Paulo, Brazil.

Methods

Radiolabeling of conjugated peptides and radiochemical evaluation. The conjugated peptides (10 μL of a μg/μL

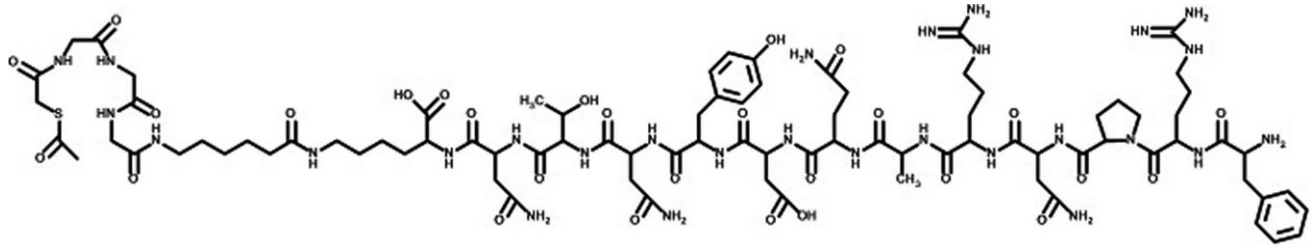

Figure 2 - Structure of conjugated DUP-1 (FRPNRAQDYNTNK) (SAMA-G-G-G-Ahx)-NH2; chemical formula: $C_{85}H_{131}N_{29}O_{27}S$; molecular weight: 2023.19.

solution) were labeled with 300 μL of technetium-99m using sodium tartrate dissolved in a labeling buffer (0.5 M ammonium bicarbonate, 0.25 M ammonium acetate, 0.18 M ammonium hydroxide, 1:1:1) along with a stannous chloride solution (chloridric acid/ascorbic acid). The reaction was induced by heating the mixture to 100°C for 20 min. Radiochemical evaluation was performed using instant thin-layer chromatography on silica gel strips, and the mobile phase consisted of methylethylketone (MEK) and a solution of 50% acetonitrile (ACN).

Each of the radiolabeled conjugates was also characterized by reverse-phase high-performance liquid chromatography analysis. All solvents used in the chromatographic analyses were HPLC-grade and had been previously filtered through 0.22-μm membrane filters (Millipore, Milford, MA, USA).

The HPLC solvents consisted of H_2O, which contained 0.1% trifluoroacetic acid (Solvent A), and ACN, which contained 0.1% trifluoracetic acid (Solvent B). The HPLC gradient system began with a solvent composition of 95% A and 5% B, which was followed by a linear gradient of 30% A and 70% B from 0 to 25 min and 5% A and 95% B from 25 to 30 min.

Determination of *log* P values. The radiotracers (100 μL) were dissolved in a mixture of equal volumes (3 mL to 3 mL) of n-octanol and water. After the mixture had been vigorously stirred and centrifuged, samples (in triplicate) from both phases (n-octanol and water) were collected and their radioactivity was measured using a gamma counter.

***In vitro* cell binding assays.** PC3 androgen-independent human prostate carcinoma cells were cultured in RPMI 1640 medium (Sigma-Aldrich, São Paulo, Brazil) that was supplemented with 10% (v/v) fetal calf serum. The cells were kept at 37°C in a humidified air environment containing 5% CO_2. They were grown to near confluency and were then harvested by trypsinization. Cells (10^6 cells/well) were seeded into six- and twelve-well culture plates for the binding studies 24 h before the experiment.

The culture plates were then filled with increasing concentrations (1 nM to 18 nM) of cold, nonlabeled conjugates along with 90 pM of ^{99m}Tc-labeled peptide and were subsequently incubated for 120 min.

Internalization studies were also performed in triplicate at 15, 30, 60, 90, and 120 min time points with and without an excess of 1 μM cold conjugated peptide for nonspecific internalization. The supernatant was collected, and cell surface-bound radioligand was removed with a two-step acid wash. Internalized radioligand was evaluated by lysing the cells with 1 M NaOH for 5 min, and radioactivity was measured with the automated γ counter.

***In vivo* studies.** All experiments were carried out in compliance with the protocol that had been approved by the local Animal Welfare Committee. Suspensions of PC3 cells (5.0×10^6) were subcutaneously injected into the upper back regions of athymic male nude mice. The tumors were allowed to grow *in vivo* for 2–3 weeks, at which point the tumor diameter was approximately 1 cm.

^{99m}Tc-conjugated peptides were injected via the tail vein into healthy Swiss mice (0.1 mL/18.5 MBq), and the biodistribution was evaluated at 5, 30, 90, and 240 min post-injection using six mice for each time point. All animals were sacrificed by cervical dislocation. Subsequently, all major organs and tissue samples were excised, weighed and counted with a NaI(Tl) gamma counter, and the percentage of the injected dose per gram of tissue was calculated using the activity of the injected dose as a standard. Biodistribution was analogously evaluated in tumor-bearing mice at 30 and 90 min post-injection and was followed by blocking studies, which involved the coinjection of excess amounts of cold conjugate.

Tumor imaging. Planar imaging studies were performed with anesthetized mice that were horizontally placed under the collimator of a Mediso Imaging System (Budapest, Hungary). A low-energy, high-resolution collimator was used, and images were acquired at 0.5 h and 1.5 h post-injection using a $256\times256\times16$ matrix size and a 20% energy window set at 140 keV for a period of 180 s.

Statistical analysis. Quantitative data were expressed as the mean ± SD. Means were compared by an independent Student's t test. *p*-values less than 0.05 were considered significant.

RESULTS

Both conjugates were radiolabeled using the same protocol. Radiolabeling with ^{99m}Tc was performed via stannous-tartrate exchange. The radiochemical purities of ^{99m}Tc-MAG_3-Ahx-BBN and ^{99m}Tc-MAG_3-Ahx-DUP-1 were $96.3\pm0.32\%$ and $96.0\pm0.15\%$, respectively, and the corresponding retention times by HPLC were 12.1 min and 13.4 min, respectively (Figure 3).

The specific activity of ^{99m}Tc-MAG_3-Ahx-BBN was 148.8 MBq/nM, and that of ^{99m}Tc-MAG_3-Ahx-DUP-1 was 224.7 MBq/nM.

The lipophilicity of the radiotracers was determined according to their proportional distribution between octanol and water. A partition ratio of 0.4065, where $log\ p = -0.39\pm0.02$, indicated moderate hydrophilicity for the ^{99m}Tc-MAG_3-Ahx-BBN. It was more remarkable for ^{99m}Tc-MAG_3-Ahx-DUP1, with a partition ratio of 0.00389 and $log\ p = -2.41\pm0.12$.

Radioactivity associated with PC3 tumor cells for ^{99m}Tc-BBN tracer was 28.87%. A sharp decrease (93%) of the binding was observed with increase of the amount of cold BBN (0 to 18 nM). For ^{99m}Tc- SAMA-G3-Ahx-DUP1 the binding value was much lower, ~ 1.97%, diminishing by a factor of 63% at the highest concentration of 18 nM (Figure 4).

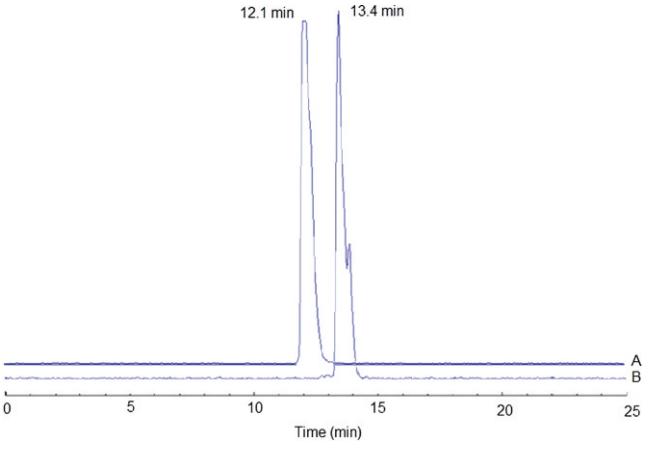

Figure 3 - Reverse-phase HPLC profile: (A) ^{99m}Tc-SAMA-G3-Ahx-BBN; (B) ^{99m}Tc- SAMA-G3-Ahx-DUP-1.

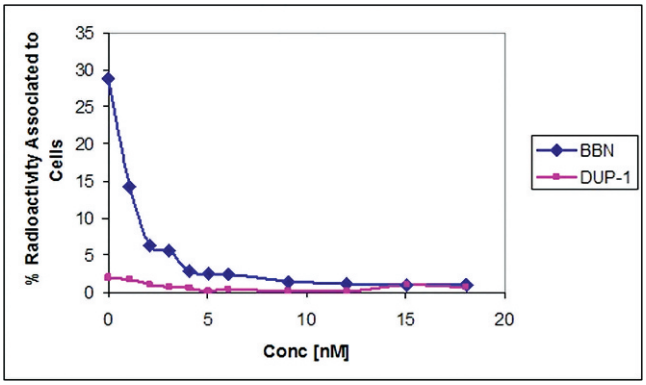

Figure 4 - Cellular uptake of the radiotracers ^{99m}Tc-SAMA-G3-Ahx-BBN and ^{99m}Tc-SAMA-G3-Ahx-DUP-1 in PC-3 human prostate carcinoma cells at 37°C. Percentage of total binding radioactivity vs. an increasing concentration of the respective cold peptide.

The internalization of the tracers by PC3 cells, as a function of time for the two radiolabeled peptide derivatives, is illustrated in Figure 5. Internalization was assessed both in the absence and presence (blocking experiments) of the native peptides.

The rate of internalization was time-dependent for ^{99m}Tc-SAMA-G3-Ahx-BBN. Incubation at 37°C resulted in an increased internalization rate, as $20.36 \pm 0.83\%$ of the radioactivity was internalized at 120 min. The internalization reached its maximum (78.32%) of total binding by 2 h. ^{99m}Tc- SAMA-G3-Ahx-DUP-1, as evaluated under the same conditions, displayed a much lower rate of internalization, which was in the range between 5.78% and 9.34% and remained stable at all time points.

The biodistribution evaluation in healthy animals confirmed that kidney uptake was more robust for the DUP tracer than for the BBN tracer ($p < 0.05$). Blood depuration was rapid and similar for both tracers ($p > 0.05$). Intestinal uptake was high and also equivalent for both radiotracers ($p > 0.05$). Hepatobiliary excretion was predominant for the BBN tracer, whereas the hepatobiliary system and the urinary system were found to be the major excretory pathways for the DUP tracer. ^{99m}Tc-SAMA-G3-Ahx-BBN exhibited greater uptake in the pancreas ($p < 0.05$) than ^{99m}Tc-SAMA-G3-Ahx-DUP-1.

Clearance from the blood and from other GRP receptor-negative tissues (heart, lung, spleen, stomach, muscle, and bone) was rapid, as less than 1% ID/g was detected 30 min after the injection of either radiotracers BBN and DUP-1 (Table 1).

The biodistribution for nude mice bearing PC3 tumors is shown in Table 2 and Figures 6 and 7. Lung uptake was in the range of 1% ID/g, and that of the heart, muscle and bone was less than 1% ID/g. Tumor uptake was not significantly different for the two radiotracers ($p > 0.05$).

The excretion profile was also investigated for the tumor-bearing mice (Figure 6). The highest level of kidney uptake for ^{99m}Tc-SAMA-G3-Ahx-DUP-1 was documented at 30 min post-injection. No differences occurred ($p > 0.05$) between blocked and unblocked animals (Figures 6 and 7).

The liver uptake of ^{99m}Tc-SAMA-G3-Ahx-BBN confirmed that tracer elimination was rapid, as the uptake values at 90 min were significantly decreased.

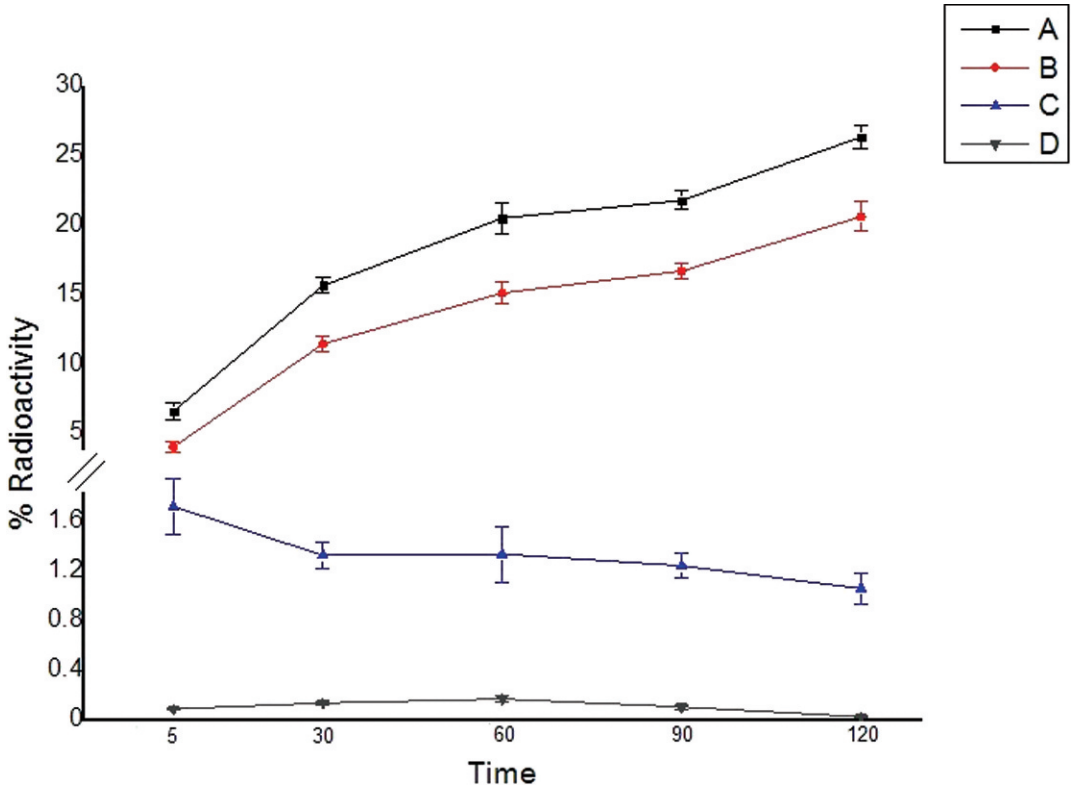

Figure 5 - Internalization of the radiotracers: total binding represents uptake on the surface membrane plus that inside of the cell; internalization represents the activity inside of the cell only. (A) Total binding – ^{99m}Tc-SAMA-G3-Ahx-BBN; (B) Internalization – ^{99m}Tc-SAMA-G3-Ahx-BBN; (C) Total binding – ^{99m}Tc- SAMA-G3-Ahx-DUP-1; (D) Internalization ^{99m}Tc- SAMA-G3-Ahx-DUP-1.

Table 1 - Biodistribution of the ^{99m}Tc conjugates in healthy *Swiss* mice.

Tissue %ID/g	Time							
	5 min		30 min		90 min		240 min	
	BBN*	DUP**	BBN*	DUP**	BBN*	DUP**	BBN*	DUP**
Blood	1.64±0.22	1.21±0.02	0.36±0.06	0.43±0.06	0.12±0.03	0.08±0.01	0.05±0.01	0.05±0.01
Heart	0.61±0.20	0.82±0.14	0.14±0.05	0.24±0.07	0.06±0.01	0.04±0.01	0.04±0.02	0.03±0.02
Lung	1.56±0.33	1.48±0.23	0.51±0.06	0.73±0.16	0.21±0.03	0.15±0.037	0.13±0.03	0.13±0.07
Kidney	1.81±0.06	22.62±2.03	3.01±0.78	21.06±0.41	0.62±0.01	7.28±2.07	0.29±0.03	3.22±0.43
Spleen	1.45±0.24	1.37±0.18	0.64±0.05	0.28±0.07	0.29±0.08	0.09±0.03	0.73±0.07	0.07±0.02
Stomach	1.49±0.20	0.73±0.17	0.49±0.05	0.91±0.11	0.83±0.32	0.27±0.01	0.67±0.05	0.29±0.01
Pancreas	6.58±1.67	1.44±0.33	2.78±0.23	0.18±0.11	1.67±0.33	0.05±0.01	0.35±0.05	0.04±0.01
Liver	10.05±2.18	12.31±2.19	2.79±0.47	8.58±1.75	1.58±0.45	1.57±0.57	1.54±0.06	1.53±0.64
L. Int.	4.17±0.77	2.92±0.24	1.00±0.22	1.11±0.07	2.00±1.21	0.33±0.28	19.40±0.9	15.45±2.8
S. Int.	12.03±3.37	16.57±3.02	14.34±2.58	13.31±4.46	18.17±2.27	14.62±2.15	0.38±0.11	1.43±0.49
Muscle	0.33±0.05	0.77±0.06	0.11±0.03	0.14±0.04	0.10±0.04	0.51±0.01	0.06±0.02	0.17±0.07
Bone	0.51±0.09	0.84±0.17	0.13±0.01	0.20±0.01	0.11±0.05	0.05±0.02	0.40±0.11	0.05±0.01

Abbreviations: L. intestine: large intestine; S. Int: small intestine;
(*)^{99m}Tc-SAMA-G3-Ahx-BBN; (**)^{99m}Tc-SAMA-G3-Ahx-DUP-1.
Data are expressed as the mean ± SD (n = 6). The radioactivity in the stomach and intestine was evaluated after thoroughly removing the luminal contents.

As shown in Figure 7, as well as in Table 2, the cold conjugate-blocked tumor uptake values for the BBN tracer were 32% and 49%, and those for the DUP tracer were 82% and 83% at 30 and 90 min post-injection, respectively. The pancreas was 93.19% blocked at 30 min and 97.06% blocked at 90 min using cold BBN, and these blockage values for the cold DUP-1 were decreased at 32.53% and 53.85%, respectively DUP-1 (Figure 7).

The scintigraphic images are shown in Figure 8. The tumor images that were acquired 90 min post-injection revealed approximately 60% less uptake than at the earlier time point. High uptake was observed in the gastrointestinal tract, and the prostate tumor was clearly visualized at 30 min post-injection. Although the image quality was somewhat better for the BBN tracer, the region of interest (ROI) measurements for both radiotracers were not significantly different ($p > 0.05$).

DISCUSSION

The radiolabeling of many peptides requires functional groups, such as spacers, chelators, or radiometals, for improved conjugation or more favorable kinetics. The preferred chelators for peptide labeling using technetium include HYNIC, the tricarbonyl core, and N_3S types, such as benzoyl or S-acetyl-MAG3 (mercaptoacetyl-Gly-Gly-Gly).

The S-acetyl group is reported to remain intact after conjugation; thus, the risk of subsequent degradation of the molecule is low (15). Degradation was not measured in the present circumstance, but it may be a useful parameter for future studies. The radiolabeling yield in this study was high, thus precluding the need for radiolabeling optimization.

Drug transportation characteristics are influenced by the partition coefficient because this coefficient affects how drugs reach the target organs and other structures at the site of action. ^{99m}Tc-SAMA-G3-Ahx-DUP-1 was more hydrophilic than ^{99m}Tc-SAMA-G3-Ahx-BBN, and this was confirmed by its stronger kidney uptake. This hydophilicity is a valuable feature of the compound that improved its solubilization and access to body systems. In the case of the prostate, too much radioactivity in the urinary system may interfere with tumor imaging; however, this limitation can be offset by simultaneous amino acid administration (6).

Table 2 - Biodistribution of the ^{99m}Tc tracers in *Nude* mice bearing PC-3 tumors.

Tissue %ID/g	Time post-injection							
	30 min				90 min			
	BBN*	BBN* Block	DUP**	DUP** Block	BBN*	BBN* Block	DUP**	DUP** Block
Blood	0.72±0.15	0.98±0.29	0.69±0.14	0.58±0.16	0.20±0.06	0.13±0.03	0.23±0.06	0.12±0.02
Heart	0.34±0.08	0.54±0.04	0.41±0.02	0.40±0.08	0.10±0.01	0.09±0.02	0.10±0.10	0.09±0.01
Lung	1.20±0.32	1.40±0.23	1.24±0.43	0.98±0.23	1.05±0.19	1.02±0.21	0.34±0.27	0.29±0.04
Spleen	1.51±0.55	1.40±0.12	0.56±0.13	0.49±0.11	0.72±0.31	0.65±0.13	0.54±0.19	0.62±0.11
Stomach	0.94±0.27	0.90±0.20	1.05±0.07	1.23±0.34	0.65±0.22	0.31±0.06	0.72±0.27	0.66±0.16
Muscle	0.27±0.09	0.30±0.03	0.27±0.27	0.23±0.03	0.25±0.04	0.16±0.03	0.31±0.11	0.28±0.03
Bone	0.50±0.12	0.78±0.13	0.31±0.08	0.27±0.02	0.24±0.08	0.29±0.02	0.30±0.05	0.24±0.02
Tumor	0.75±0.15	0.51±0.17	0.85±0.19	0.15±0.03	0.29±0.05	0.16±0.02	0.41±0.11	0.07±0.01
Uptake ratio (tumor/normal tissue)								
Tumor/blood	1.04		1.23		1.45		1.78	
Tumor/muscle	2.78		3.15		1.16		1.32	

(*)^{99m}Tc-SAMA-G3-Ahx-BBN; (**)^{99m}Tc-SAMA-G3-Ahx-DUP-1. The data are expressed as the mean ± SD (n = 6).

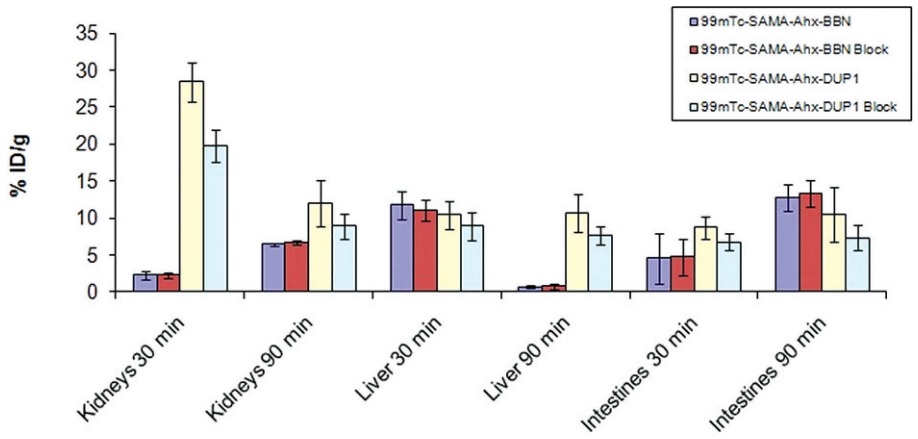

Figure 6 - Excretion organ uptake of ^{99m}Tc- peptides in urethane-anesthetized mice (0.1 mL/18.5 MBq).

PC3 human prostate cancer cells overexpress gastrin-releasing peptide receptor (GRPR), which renders them an attractive target for bombesin markers. Schally and co-workers have shown that there are 44,000 bombesin receptor sites/cell on PC-3 human prostate cancer cells (16).

Zitzmann et al. (11) used a 12-mer M13 phage display peptide library to screen for ligands of the DU-145 prostate carcinoma cell line, as well as those of PC3 cells. After six rounds of biopanning, all sequenced phage clones were found to display the same peptide, FRPNRAQDYNTN (DUP-1). The number of cell receptors for this molecule has not been estimated. Nevertheless, the Zitzman group (11) validated the binding of DUP-1 to PC-3 cells using a radioactive derivative of DUP-1 in the presence of increasing concentrations of unlabeled DUP-1 (17).

Cell binding assays in the current study were consistent with the higher affinity of the BBN tracer. For DUP-1, maximum binding and internalization were reached after 5 min and subsequently decreased over time. A comparable profile of cell binding and internalization has been described for ^{131}I-DUP-1 regarding DU-145 and PC3 tumor cells (11).

Such differences between BBN and DUP-1 may be partially explained by the fact that the DUP-1 conjugate has twice the molecular weight and a greater hydrophilicity than BBN. Degradation was not considered to be a problem in this study, as higher rather than lower blood concentrations tend to occur in such circumstances. The BBN concentration in the pancreas was also significantly greater, which is in accordance with the literature. The pancreas has

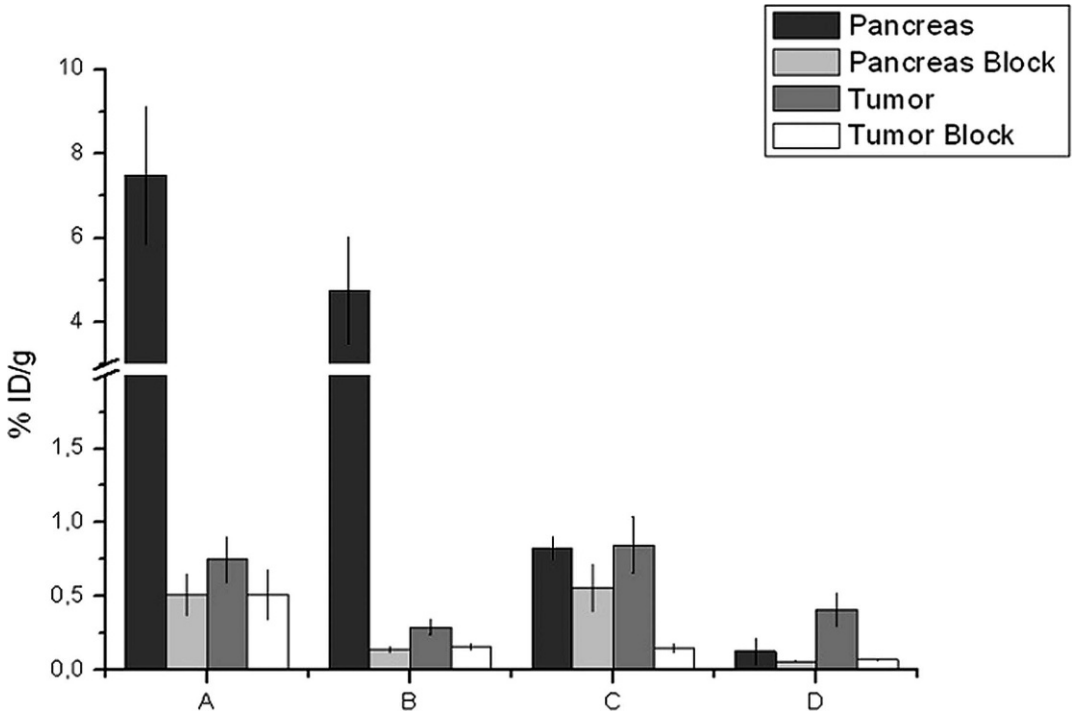

Figure 7 - Pancreatic and tumor uptake in regular, as well as blocked, urethane-anesthetized animals (0.1 mL/18.5 MBq): (A) ^{99m}Tc-SAMA-G3-Ahx-BBN 30 min; (B) ^{99m}Tc-SAMA-G3-Ahx-BBN 90 min; (C) ^{99m}Tc-SAMA-G3-Ahx-DUP 30 min; (D) ^{99m}Tc-SAMA-G3-Ahx-DUP 90 min.

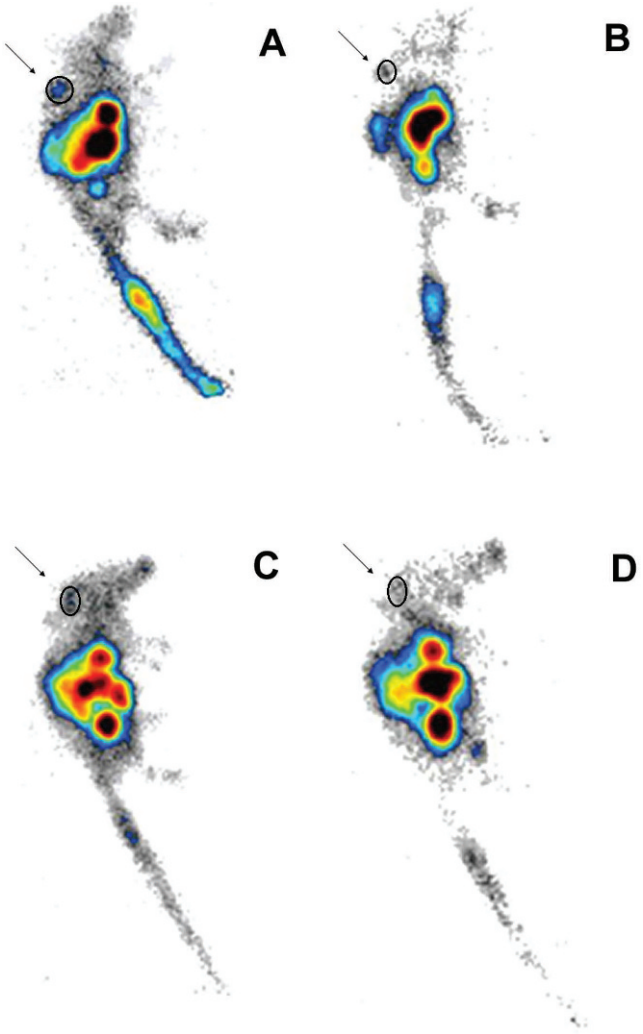

Figure 8 - Lateral scintigraphic images of urethane-anesthetized mice bearing PC3 tumors in the upper right part of the back; (A) ^{99m}Tc-SAMA-G3-Ahx-BBN – 30 min (ROI: 0.49%); (B) ^{99m}Tc-SAMA-G3-Ahx-BBN – 90 min (ROI: 0.26%); (C) ^{99m}Tc-SAMA-G3-Ahx-DUP-1 – 30 min (ROI: 0.71%; (D) ^{99m}Tc-SAMA-G3-Ahx-DUP-1 – 90 min (ROI: 0.27%) using a 256×2 or 56×16 matrix size (0.1 mL/18.5 MBq).

long been known to express a large number of GRP receptors (18). Indeed, this number is approximately eightfold greater than that of PC3 tumors (18). These properties of BBN suggest that this peptide will likely remain the first choice for prostate cancer, although this does not rule out interest in alternative agents.

The chosen time (30 min) for the evaluation of the tumor-bearing mice was based on blood clearance. Blood elimination was conveniently rapid and demonstrated an uptake of less than 0.5% ID/mL. However, the optimal time for the BBN diagnosis was 90 min post-injection. Our preliminary conjugation of the molecule probably improved its stability, compared to the study of Zitzmann et al. (11) that demonstrated decreased blood uptake.

DUP-1 evaluation times for the tumors were less ideal. The highest cell binding values occurred as early as 5 min after incubation. By 30 min, the DUP-1 tracer, which has been shown to bind very quickly, may have already been washed out. Also, Askoxylakis et al. (12) observed elevated ^{131}I-DUP tumor uptake at the relatively early time of 15 min. Thus, future studies should begin assessments at earlier time-points to disclose stronger cell affinities and higher concentrations than were reported here. In addition, binding affinity was reduced in the study by Askoxylakis et al., which evidenced the difficulties associated with reaching an ideal molecular design. These authors concluded that the sequence in the middle of the NRAQDY molecule may be significant for target binding.

The occurrence of instability and degradation was suggested by Askoxylakis et al., but this was not in agreement with the findings of others. Phage display peptides have been used as vehicles for the delivery of drugs and other biomolecules, and they have achieved high success due to their affinity and selectivity for a variety of cellular targets. Attention to peptide conformation and the chemical synthesis of specific molecules have been cited as the greatest potential challenges for this technique (19,20). As a result, stability studies were not considered a priority in the current investigation.

Functional groups are crucial for the optimization of peptide tracers, and this also applies to DUP-1. Accordingly, the glycosylation state of the peptide and the effects of various chelators need to be assessed by future studies.

Both the BBN and DUP-1 tracers exhibited low but consistent tumor uptake. The DUP-1 tumor uptake values likely experienced interference due to the experimental design, as peak values were missed at the comparatively long analysis interval of 30 min. Improvements in the design of the molecule, which may result in more favorable pharmacokinetics, along with the use of a shorter assessment timeframe may substantially enhance the potential of DUP-1 to be used as a prostate tumor radiopeptide.

ACKNOWLEDGMENTS

We are grateful to Rodrigo Teodoro and Natanael Gomes da Silva for their technical support during the animal experiments and imaging procedures. We also thank Roselaine Campos Targino for her help concerning cell culture and Maria Neide Ferreira Mascarenhas for her cooperation regarding the animal facilities.

AUTHOR CONTRIBUTIONS

Faintuch BL, Nanda PK, and Smith CJ designed the protocol and analyzed the results, and all the authors examined and approved the final manuscript. Oliveira EA, Nunez EGF, and Moro AM prepared the materials and conducted the technical procedures.

REFERENCES

1. Yang M, Gao H, Zhou Y, Ma Y, Quan Q, Lang L, et al. 18F-labeled GRPR agonist and antagonists: A comparative study in prostate cancer imaging. Theranostics. 2011;1:220-9.
2. González N, Mantey SA, Pradhan TK, Sancho V, Moody TW, Coy DH, et al. Characterization of putative GRP-and NMB-receptor antagonists interaction with human receptors. Peptides. 2009;30:1473-86, http://dx.doi.org/10.1016/j.peptides.2009.05.007.
3. Markwalder R, Reubi JC. Gastrin-releasing peptide receptors in the human prostate relation to neoplastic transformation. Cancer Res. 1999;59:1152-9.
4. Beer AJ, Eiber M, Souvatzoglou M, Schwaiger M, Krause BJ. Radionuclide and hybrid imaging of recurrent prostate cancer. Lancet Oncol. 2011;12:181-91, http://dx.doi.org/10.1016/S1470-2045(10)70103-0.
5. Nanda PK, Lane SR, Retzloff LB, Pandey US, Smith CJ. Radiolabeled regulatory peptides for imaging and therapy. Curr Opin Endocrinol Diabetes Obes. 2010;17:69-76.

6. Faintuch BL, Teodoro R, Duatti A, Muramoto E, Faintuch S, Smith CJ. Radiolabeled bombesin analogs for prostate cancer diagnosis: preclinical studies. Nucl Med Biol. 2008;35:401-11, http://dx.doi.org/10.1016/j.nucmedbio.2008.02.005.
7. Flores DG, Lenz G, Roesler R, Schwartzmann G. Gastrin-releasing peptide receptor signaling in cancer. Cancer Therapy. 2009;7:332-46.
8. Ferro-Flores G, Rivero IA, Santos-Cuevas CL, Sarmiento JI, Arteaga de Murphy C, Ocampo-García BE, et al. Click chemistry for [99mTc(CO)3] labeling of Lys3-bombesin. Appl Radiot Isot. 2010;68:2274-8, http://dx.doi.org/10.1016/j.apradiso.2010.06.014.
9. Parry JJ, Andrews R, Rogers BE. MicroPET imaging of breast cancer using radiolabeled bombesin analogs targeting the gastrin-releasing peptide receptor. Breast Cancer Res Treat. 2007;101:175-83, http://dx.doi.org/10.1007/s10549-006-9287-8.
10. Krumpe LRH, Mori T. Potential of phage-displayed peptide library technology to identify functional targeting peptides. Expert Opin Drug Discov. 2007;2:525-43, http://dx.doi.org/10.1517/17460441.2.4.525.
11. Zitzmann S, Mier W, Schad A, Kinscherf R, Askoxylakis V, Kraemer S, et al. A new prostate carcinoma binding peptide (DUP-1) for tumor imaging and therapy. Clin Cancer Res. 2005;11:139–46.
12. Askoxylakis V, Zitzmann-Kolbe S, Zoller F, Altmann A, Markert A, Rana S, et al. Challenges in optimizing a prostate carcinoma binding peptide, identified through the phage display technology. Molecules. 2011;16:1559-78, http://dx.doi.org/10.3390/molecules16021559.
13. Bartoloma M, Valliant J, Maresca KP, Babich J, Zubieta J. Single amino acid chelates (SAAC): a strategy for the design of technetium and rhenium radiopharmaceuticals. Chem Commun. 2009;7:493-512, http://dx.doi.org/10.1039/b814903h.
14. Reile H, Armatis PE, Schally AV. Characterization of high-affinity receptors for bombesin/gastrin releasing peptide on the human prostate cancer cell lines PC-3 and DU-145: Internalization of receptor bound 125I-(Tyr4) bombesin by tumor cells. Prostate. 1994;25:29–38, http://dx.doi.org/10.1002/pros.2990250105.
15. Liu G, Hnatowich DJ. Labeling biomolecules with radiorhenium: a review of the bifunctional chelators. Anticancer Agents Med Chem. 2007;7:367-77, http://dx.doi.org/10.2174/187152007780618144.
16. Byk G, Partouche S, Weiss A, Margel S, Khandadash R. Fully Synthetic Phage-Like System for Screening Mixtures of Small Molecules in Live Cells. J Comb Chem. 2010;12:332–45, http://dx.doi.org/10.1021/cc900156z.
17. Deschodt-Lanckman M, Robberecht P, De Neef P, Lammens M, Christophe J. In vitro action of bombesin and bombesin-like peptides on amylase secretion, calcium efflux, and adenylate cyclase activity in the rat pancreas: a comparison with other secretagogues. J Clin Invest. 1976;58:891–8, http://dx.doi.org/10.1172/JCI108542.
18. Chanda N, Kattumuri V, Shukla R, Zambre A, Katti K, Upendran A, et al. Bombesin functionalized gold nanoparticles show in vitro and in vivo cancer receptor specificity. Proc Natl Acad Sci USA. 2010;107:8760-5, http://dx.doi.org/10.1073/pnas.1002143107.
19. Min K, Jo H, Song K, Cho M, Chun YS, Jon S, et al. Dual-aptamer-based delivery vehicle of doxorubicin to both PSMA (+) and PSMA (-) prostate cancers. Biomaterials. 2011;32:2124-32, http://dx.doi.org/10.1016/j.biomaterials.2010.11.035.
20. Uchiyama F, Tanaka Y, Minari Y, Tokui N. Designing scaffolds of peptides for phage display libraries. J Biosci Bioeng 2005;99:448-56.